scientific reports

Check for updates

OPEN

Energy transfer through third-grade fluid flow across an inclined stretching sheet subject to thermal radiation and Lorentz force

Najiba Hasan Hamad[1], Muhammad Bilal[2], Aatif Ali[3], Sayed M. Eldin[4], Mohamed Sharaf[5] & Mati Ur Rahman[3,6]✉

The heat and mass transfer through the third grade fluid (TGF) flow over an inclined elongating sheet with the consequences of magnetic field and chemical reaction is reported. The impact of activation energy, heat source/sink, and thermal radiation is considered on the TGF flow. Fluid that demonstrate non-Newtonian (NN) properties such as shear thickening, shear thinning, and normal stresses despite the fact that the boundary is inflexible is known as TGF. It also has viscous elastic fluid properties. In the proposed model, the TGF model is designed in form of nonlinear coupled partial differential equations (PDEs). Before employing the numerical package bvp4c, the system of coupled equations are reduced into non-dimensional form. The finite-difference code bvp4c, in particular, executes the Lobatto three-stage IIIa formula. The impacts of flow constraints on velocity field, energy profile, Nusselt number and skin friction are displayed through Tables and Figures. For validity of the results, the numerical comparison with the published study is performed through Table. From graphical results, it can be perceived that the fluid velocity enriches with the variation of TGF factor and Richardson number. The heat source parameter operational as a heating mediator for the flow system, its influence enhances the fluid temperature.

List of symbols

U_w	Sheet stretching velocity
qr	Thermal radiation
K_0	Surface penetrability
Ea	Activation energy
F	Inertia constant
ν	Kinematic viscosity
α_m	Thermal diffusivity
μ	Dynamic viscosity
D_m	Mass diffusivity
N	Buoyancy ratio factor
M	Magnetic factor
g	Gravitational acceleration
T_w	Surface temperature
NN	Non-Newtonian
δ	Electrical conductivity
$(\alpha_1,\beta_3,\alpha_2)$	Material moduli
Q_0	Heat source
$B(x)$	Magnetic field

[1]Building and Construction Department, Shaqlawa Technical College, Erbil Polytechnic University, Erbīl, Iraq. [2]Sheikh Taimur Academic Block-II, Department of Mathematics, University of Peshawar, Peshawar 25120, Khyber Pakhtunkhwa, Pakistan. [3]School of Mathematical Sciences, Jiangsu University, Zhenjiang 212013, Jiangsu, China. [4]Center of Research, Faculty of Engineering, Future University in Egypt, New Cairo 11835, Egypt. [5]Industrial Engineering Department, College of Engineering, King Saud University, P.O. Box 800, 11421 Riyadh, Saudi Arabia. [6]Department of Computer Science and Mathematics, Lebanese American University, Beirut, Lebanon. ✉email: MatiUr.Rahman@lau.edu.lb

C_p	Specific heat competence
k_r	Chemical reaction
Ri	Richardson number
L	Viscoelastic factor
K^*	Permeability factor
β	Third-grade fluid factor
R	Chemical reaction factor
C_w	Surface concentration
MHD	Magnetohydrodynamics
TGF	Third grade fluid

The fluid flow through a stretching sheet holds substantial significance within the domain of fluid dynamics, owing to its wide array of uses in various engineering and industrial domains. Abolbashari et al.[1] analytically examined the behavior of fluid flow. Their study focused on a flow scenario where a stretching sheet was involved with velocity slip condition. Zeeshan et al.[2] deliberated the heat transmission on the motion of a ferromagnetic fluid over an extending surface. This ferromagnetic fluid consisted of a well-blended mixture of magnetic solid particles all of this occurs in the presence of an electromagnetic dipole state. Shit et al.[3] conducted a study that explored the dynamics of unsteady boundary layer magnetohydrodynamic flow and convective heat source. Sandeep and Sulochana[4] developed a new mathematical model to investigate energy and heat transmission in non-Newtonian fluids on a stretched surface. Results showed that the Jeffrey nanofluid outperformed Maxwell and Oldroyd-B nanofluids in terms of heat transfer. Besthapu et al.[5] conducted an examination of velocity slip on a extending sheet with convectively non-uniform characteristics. Alqahtani et al.[6] conducted a 3D simulation on MHD behavior of hybrid fluid flow across double stretching surfaces. Chu et al.[7] investigated a 2D continuous laminar movement of a TGF past a flow over a shrinking surface containing gyrotactic microorganisms. The flow was electrically conductive due to an applied electric field and the Buongiorno nanoliquid model was used for mathematical modeling. The study also incorporated chemical reactions with activation energy effects. Kumar et al.[8] and Li et al.[9] investigated the energy transmission rate in a hydromagnetic Williamson nanoliquid flow thru a absorbent strained sheet. Khan et al.[10] conducted a discussion on the hybrid nanoliquid flow consisting of Cu and Al_2O_3 nanoparticles in water. This flow occurred from a centrifugally porous surface that could either shrink or stretch. Elattar et al.[11] scrutinized the steady flow of hybrid nanoliquid over an impermeable stretchable sheet. A mathematical model was developed with the aim of improving the rates of energy transference, enhancing the efficiency and effectiveness of thermal energy propagation. Dogonchi et al.[12] described the entropy and thermal analyses of the nanoliquid flow within a porous cylinder. Some remarkable results recently presented by Ref.[13–18].

The flow of a mixture of fluid and solid particles is inherently complex and can be influenced by numerous variables. To better understand and study these intricate flows, one common approach is to treat the mixture as a NN fluid. Considerable research has been dedicated to the analysis of various transport phenomena occurring within non-Newtonian fluids, including substances like coal slurries. Among these processes, heat transfer is of particular significance in the context of handling and processing these fluids. It plays a pivotal function in the efficient management and treatment of such complex mixtures[19]. Ariel[20] conducted a study on the laminar flow and steady of a TGF over a permeable flat conduit. Ellahi and Riaz[21] carried out an investigation to examine the TGF with changing viscosity in a conduit. This study also considered the heat diffusion features of the fluid in the context of the analysis. Bilal et al.[22] explored the MHD motion of Carreau Yasuda liquid initiated by an exponentially extending surface. Adesanya et al.[23] performed a study on the intrinsic irreversibility linked with the motion of third-grade fluid through a conduit exposed to convective heating. This study recognizes that the heat generated leads to continuous entropy generation within the channel. Reddy et al.[24] conducted an investigation to understand the effect of the Prandtl number on TGF around a vertically oriented cylinder that is uniformly heated. Mahanthesh and Joseph[25] examined the steady-state behavior of third-grade liquid flowing over a pressure-type die in the existence of nanoparticles. The fluid is dissipative and its properties are considered to be constant throughout the analysis. Contemporary and innovative literature concerning Non-Newtonian (third-grade fluid) can be found in Refs.[26–30].

Magnetohydrodynamics (MHD) is the discipline that analyzes the behavior of electrically conductive substances including plasmas, ionized gases and liquid metals when subjected to magnetic fields. This area of research investigates the interaction between fluid motion and electromagnetic forces and it possesses extensive applications in geophysics, engineering, plasma physics and astrophysics. The impact of fluctuating viscous flow within a narrowing channel was scrutinized by Al-Habahbeh et al.[31]. Rashidi et al.[32] provided an extensive overview of the utilization of MHD and biological systems. The investigation of MHD fluid motion in diverse orientations linked to human anatomical structures is a significant scientific domain given its relevance and applications in the field of medical sciences. Ellahi et al.[33] examined the concurrent impacts of MHD, heat transfer and slip over a flat plate in motion. Furthermore, this study also assessed the influence of entropy generation within this context. Lv et al.[34] explored the effects of various physical phenomena, including diffusion-thermo, radiation-absorption in the context of MHD free convective spinning flow of nanoliquids. Kumam et al.[35] studied the MHD Radiative unsteady fluid flow with the upshot of heat source across a channel placed in absorbent medium. Tian et al.[36] studied the energy transfer though fluid flow surrounded by a rectangular enclosure having a heat sink filled with hybrid nanofluids and the exploration focused on the joint effects of forced and natural convection. Bhatti et al.[37] conducted research into the unsteady flow within the confines of parallel spinning spherical disks placed in a permeable medium. The influence of magnetization on lubrication had attracted consideration due to their important roles in various industrial applications. One notable example was their increased use in high-temperature bearings with liquid metal lubricants. Alharbi et al.[38] carried out a computational examination of the

influence of different geometric factors on an extending cylinder. Hamid and Khan[39] investigated the upshot of magnetic flux on NN Williamson fluid flow. The flow was induced by an elongating cylinder in the existence of nanocomposites. Shamshuddin et al.[40] studied the upshot of chemical reactions Couette-Poiseuille nanoliquid flow through a gyrating disc. Kumam et al.[41] explored the MHD unsteady radiative flow. Khan and Alzahrani[42] focused on optimizing entropy and understanding heat transport in the flow of a magneto-nanomaterial. This investigation took into account the influence of MHD within the fluid. Adnan and Ashraf[43] and Li et al.[44] evaluated the nanoliquid flow across a permeable surface.

The originality of the proposed model is to examine the heat and mass transfer through the TGF flow over an inclined elongating sheet. The impact of magnetic field, activation energy and thermal radiation is considered on the TGF flow. Fluid that demonstrate NN properties such as shear thickening, shear thinning, and normal stresses despite the fact that the boundary is inflexible is known as TGF. In the proposed model, the TGF model is conveyed in form of nonlinear coupled PDEs. Before employing the numerical package bvp4c, the system of coupled equations are reduced into non-dimensional form. The significances of flow factors on velocity field, energy profile and Nusselt number are presented through Tables and Figures. For validity of the results, the numerical comparison with the published existing study is performed through Table. In the upcoming section, the problem is designed in form of PDEs and numerically solved.

Formulation of the problem

We have considered the mass and energy transfer through the steady and incompressible flow TGF over an inclined elongating sheet. The two-dimensional TGF flow is inspected under the impacts of chemical reaction, magnetic field, activation energy and thermal radiation. The surface of the sheet is assumed to be Darcy permeable. The x-axis and y-axis is the horizontal and normal axis to an inclined stretching sheet as shown in Fig. 1. Here, g, T_w and C_w is the gravitational acceleration, surface temperature and concentration respectively. By keeping in view, the above suppositions, the TGF flow equations are expressed as[45,46]:

$$\frac{\partial u}{\partial x}+\frac{\partial u}{\partial x}=0, \tag{1}$$

$$\left.\begin{aligned} u\frac{\partial u}{\partial x}+v\frac{\partial u}{\partial y}=\nu\frac{\partial^2 u}{\partial y^2}+\frac{\alpha_1}{\rho}\left(u\frac{\partial^3 u}{\partial y\partial x}+\frac{\partial u}{\partial x}\left(\frac{\partial^2 u}{\partial y^2}\right)+3\frac{\partial u}{\partial y}\left(\frac{\partial^2 u}{\partial y^2}\right)+v\frac{\partial^3 u}{\partial y^3}\right)+2\frac{\alpha_1}{\rho}\frac{\partial u}{\partial y}\left(\frac{\partial^2 u}{\partial y^2}\right)+6\beta_3\\ \left(\frac{\partial u}{\partial y}\right)\left(\frac{\partial^2 u^2}{\partial y^2}\right)+g(T-T_\infty)\beta_T\cos\alpha+g(C-C_\infty)\beta_c\cos\alpha-\frac{\alpha B(x)^2}{\rho}-\frac{uv}{K_0}-Fu^2, \end{aligned}\right\} \tag{2}$$

$$u\frac{\partial T}{\partial x}+v\frac{\partial T}{\partial y}=\alpha\frac{\partial^2 T}{\partial y^2}+\frac{Q_0}{\rho C_p}(T-T_\infty)-\frac{1}{\rho C_p}\frac{\partial qr}{\partial y}, \tag{3}$$

$$u\frac{\partial C}{\partial x}+v\frac{\partial C}{\partial y}=D_m\frac{\partial^2 C}{\partial y^2}-k_r^2(C-C_0)\left(\frac{T}{T_\infty}\right)^n\exp\left(-\frac{E_a}{\kappa T}\right). \tag{4}$$

Boundary conditions (BCs) are[45]:

$$\left.\begin{aligned} u=U_w=U_0e^{\frac{x}{L}},\ C=C_w(x)=C_\infty+C_0e^{\frac{x}{L}},\ T=T_w(x)=T_\infty+C_0e^{\frac{x}{L}},\ v=0\ \text{ at }\ y\to 0\\ u\to 0,\ C\to C_\infty,\ T\to T_\infty\ \text{ at }\ y\to\infty. \end{aligned}\right\} \tag{5}$$

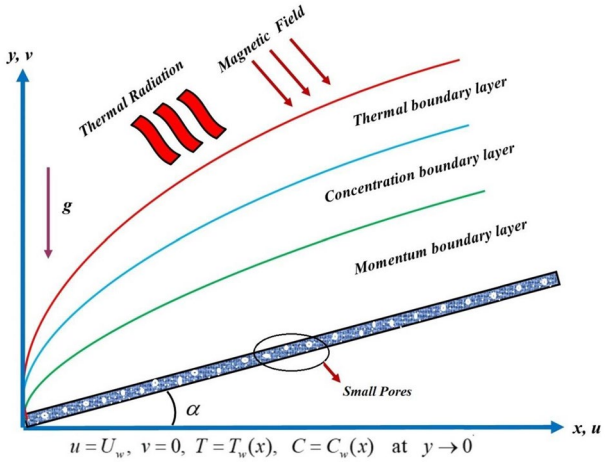

Figure 1. TGF flow across a stretching inclined surface.

Here, $(\alpha_1,\beta_3,\alpha_2)$ are the moduli of material. U_w and δ is the sheet stretching velocity and electrical conductivity, $qr = -\frac{4\sigma^*}{3k^*}\frac{\partial T^4}{\partial y}$,$K_0$ and Q_0 is the thermal radiation, surface penetrability and heat source. $B(x) = B_0 e^{\frac{x}{L}}$ and Ea is the magnetic field and activation energy, k_r and C_p is the chemical reaction and specific heat competence, $F = \frac{C_b}{\sqrt{K_0}}$,$\nu$ and μ is the inertia constant, kinematic and dynamic viscosity, α_m and D_m is the mass and thermal diffusivity.

In order to simplify Eqs. (2)–(4) and (5) to nonlinear ODEs, we use the following makeover as[39]:

$$u = U_0 e^{\frac{x}{L}}, v = \sqrt{\frac{\nu U_0}{2L}}\left(f(\eta)) + \eta f'(\eta)\right)e^{\frac{x}{L}},\ \ \eta = \sqrt{\frac{U_0}{2L\nu}}ye^{\frac{x}{L}},\ \ T = T_\infty + C_0 e^{\frac{x}{L}},\ \ C_w = C_\infty + C_0 e^{\frac{x}{L}}. \quad (6)$$

By using Eq. (6), we get:

$$\begin{aligned} &f''' + ff'' - 2f'^2 + 2R_i(\theta + N\phi)\cos\alpha + K\left(6f'f''' - 2\eta\left(f''\right)f'''' - 9f''^2\right) \\ &-L\left(3\left(f''\right)^2 + \eta\left(f''\right)f''''\right) + 3Re\,\beta\left(f''\right)^2 f''' - Mf' - K^*f' - Fr\left(f'\right)^2 = 0, \end{aligned} \quad (7)$$

$$(1 + Rd)\theta'' - Prf'\theta + Prf\theta' + Hs\theta = 0, \quad (8)$$

$$\frac{1}{Sc}\phi'' + f\phi' - f'\phi - Sc\,R(1 + \delta\Theta)^n\varphi\ \exp\left(-\frac{E}{1 + \delta\Theta}\right) = 0. \quad (9)$$

Transform BCs are:

$$\left.\begin{aligned} &f'(\eta) = 1,\ \phi(\eta) = 1,\ \theta(\eta) = 1,\ f(\eta) = 0\ \ \text{as}\ \ \eta \to 0 \\ &f'(\eta) \to 0,\ \ f''(\eta) \to 1,\ \theta(\eta) \to 1,\ \phi(\eta) \to 0\ \ \text{as}\ \ \eta \to \infty. \end{aligned}\right\} \quad (10)$$

The constraints derived from Eqs. (7)–(9) are given in Table 1.

The Nusselt number, drag force, Sherwood number are:

$$Nu = \frac{q_w x}{k(T - T_\infty)},\ \ C_f = \frac{\tau_w}{\rho U_w^2},\ \ Sh = \frac{q_m x}{D_m(C - C_\infty)}. \quad (11)$$

where

$$\begin{aligned} \tau_w &= \left(\frac{\partial u}{\partial y} + \frac{\alpha_1}{\mu}\left(2\frac{\partial u}{\partial x}\left(\frac{\partial u}{\partial y}\right) + u\frac{\partial^2 u}{\partial y \partial x} + v\frac{\partial^2 u}{\partial y^2}\right) + \frac{2\beta_3}{\mu}\left(\frac{\partial u}{\partial y}\right)^2\right) \\ q_w &= -\left(\frac{\partial T}{\partial y}\right)k,\ \ q_m = -\left(\frac{\partial C}{\partial y}\right)D_m\ \ \text{at}\ \ y = 0. \end{aligned} \quad (12)$$

Parameters	Symbols	Expression
Richardson number	Ri	$Ri = \frac{Gr}{\mathrm{Re}^2}$
Buoyancy ratio factor	N	$N = \frac{B_c C_0}{\mathrm{Re}^2}$
Viscoelastic factor	L	$L = \frac{\alpha_2 U_0 e^{\frac{x}{L}}}{2\rho\nu L}$
Third-grade fluid factor	β	$\beta = \frac{\beta_2 U_0 e^{\frac{x}{L}}}{\rho\nu L}$
Cross viscous term	K	$K = \frac{\alpha_1 U_0 e^{\frac{x}{L}}}{\mathrm{Re}^2}$
Permeability factor	K^*	$K^* = \frac{2\nu L}{k_1 U_0 e^{\frac{x}{L}}}$
Magnetic factor	M	$M = \frac{2\delta\beta_0^2}{\rho U_0}$
local inertial constant	Fr	$Fr = \frac{2C_b L}{\sqrt{k_0}}$
Prandtl number	Pr	$Pr = \frac{\nu}{\alpha}$
Activation energy	E	$E = \frac{E_a}{\kappa T_\infty}$,
Schmidt number	Sc	$Sc = \frac{\nu}{D_m}$
Chemical reaction factor	R	$R = \frac{k_r^2}{c}$
Heat source term	Q_e	$Q_e = \frac{Q_0}{\rho C_p a}$
Grashof number	Gr	$Gr = \frac{g\beta_T(T_w - T_\infty)L^3}{2}$
Reynold number	Re	$Re = \frac{U_0 L}{\nu}$

Table 1. The list of dimensionless parameters.

The dimensionless form of Eq. (11) is:

$$C_{fL} = \frac{2}{\sqrt{Re_L}}\left(K\left(3f'(0)f''(0) - f''(0)f(0)\right) + 2\beta Re_x f''^2(0) + f''(0)\right),$$
$$Re_L^{-\frac{1}{2}} Nu_L = -\theta(0), \quad Re_L^{-\frac{1}{2}} Sh_L = -\varphi(0). \tag{13}$$

Numerical solution and validation of the problem

The solutions of [Eqs. (7)–(9)] and its BCs [Eq. (10)] are derived in this section. The outcomes are accomplished by engaging the MATLAB code "bvp4c" (built-in package). The bvp4c package is built on the Lobatto III principle[47–49]. Before, solving the Eqs. (7)–(9) and Eq. (10), it must be transformed into first order system of ODEs. The transformation procedure is as follow:

$$\Re_1 = f, \quad \Re_2 = f', \quad \Re_3 = f'', \quad \Re_4 = \theta, \quad \Re_5 = \theta', \quad \Re_6 = \phi, \quad \Re_7 = \phi'. \tag{14}$$

By placing Eq. (14) in Eqs. (7)–(9) and (10) to get:

$$\Re_3' + \Re_1\Re_3 - 2\Re_2^2 + 2R_i(\Re_4 + N\Re_6)\cos\alpha + K\left(6\Re_2\Re_3' - 2\eta\Re_3\Re_3' - 9\Re_3^2\right) - L\left(3\Re_3^2 + \eta\Re_3\Re_3'\right) + 3\beta Re\Re_3^2\Re_3' - K^*\Re_2 - M\Re_2 - Fr\Re_2^2 = 0, \tag{15}$$

$$(1 + Rd)\Re_5' - Pr\,\Re_2\Re_4 + Pr f\Re_5 + Q_e\,\Re_4 = 0, \tag{16}$$

$$\frac{1}{Sc}\Re_7' + \Re_1\Re_7 - \Re_2\,\Re_6 - Sc\,R(1 + \delta\,\Re_4)^n\Re_6\ \exp\left(-\frac{E}{1 + \delta\,\Re_4}\right) = 0. \tag{17}$$

The BCs are:

$$\left.\begin{array}{l}\Re_1(\eta) = 0, \ \Re_2(\eta) = 1, \ \Re_4(\eta) = 1, \ \Re_6(\eta) = 1 \ \text{ as } \ \eta \to 0\\ \Re_2(\eta) \to 0, \ \Re_3(\eta) \to 1, \ \Re_4(\eta) \to 1, \ \Re_6(\eta) \to 0 \ \text{ as } \ \eta \to \infty.\end{array}\right\} \tag{18}$$

Table 2 displays the numerical estimation of the present study with the existing works. It has been observed that the present results are precise and consistent.

Results and discussion

We have calculated the mutual effect of magnetic force and chemical reaction on the energy and mass conduction through the TGF across a stretching sheet.

Figures 2, 3, 4, 5 and 6 revealed the effect of Richardson number Ri, TGF factor β, magnetic factor M, permeability factor K^* and local inertial constant Fr versus $f'(\eta)$. Figures 2 and 3 reports that the velocity curves develop for the rising values of Richardson number Ri and third-grade fluid factor. Richardson number is the ration between Grashof and Reynold number. The Reynold number has an transposed relation with Ri, therefore the fluid velocity $f'(\eta)$ improves with the variation of Ri. Similarly, the action of third-grade fluid factor β also enhances the velocity as presented in Fig. 3. Physically, the kinetic viscosity drops, while the stretching velocity of fluid develops with the effect of β, which results in such scenario. The influence of magnetic factor M, permeability factor K^* and local inertial constant Fr, all diminish the fluid velocity as publicized in Figs. 4, 5 and 6. Physically, the resistive force opposes the fluid velocity $f'(\eta)$, which is produced due to magnetic effect (Fig. 4). On the other hand, the rising permeability of the sheet resists to the flow field, which causes in the reducing of velocity field (Fig. 5). The consequences of inertial forces also decline the velocity curve $f'(\eta)$ as exposed in Fig. 6.

Figures 7, 8 and 9 highlight the significances of Prandtl number, Rd and Q_e on the energy $\theta(\eta)$ field. Figure 7 exposes that the temperature curve drops with the effect of Prandtl number. Physically, the thermal diffusivity of higher Prandtl fluid is less, that's why, the effect of Pr drops the energy field (Fig. 7). The radiation effect transfers thermal energy form heat source to the system, which results in the elevation of temperature field $\theta(\eta)$ (Fig. 8). Similarly, the heat source working as heating agent for the flow system, there effect rises the fluid temperature $\theta(\eta)$, as displayed in Fig. 9. Figures 10 and 11 highlights the significances of activation energy E, R and Schmidth number Sc on the mass profile $\phi(\eta)$. Figures 10 and 11 explained that activation energy factor and

Pr	Magyari and Keller[50]	Abbas et al.[45]	Present study
1.0	0.9446	0.9452	0.945267
3.0	1.8590	1.8522	1.852283
5.0	2.5100	2.5175	2.517585
10	3.6503	3.6567	3.656832

Table 2. Numerical evaluation of the present study with the existing works, while taking $M = 0,\ Ri = 0,\ L = 0,\ Sc = 0,\ Fr = 0,\ K^* = 0$.

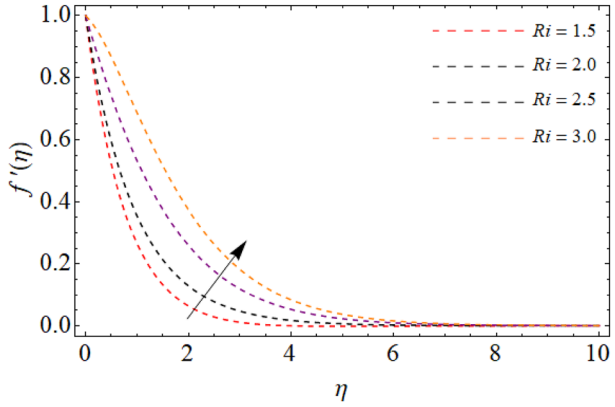

Figure 2. Velocity $f'(\eta)$ versus Richardson number Ri.

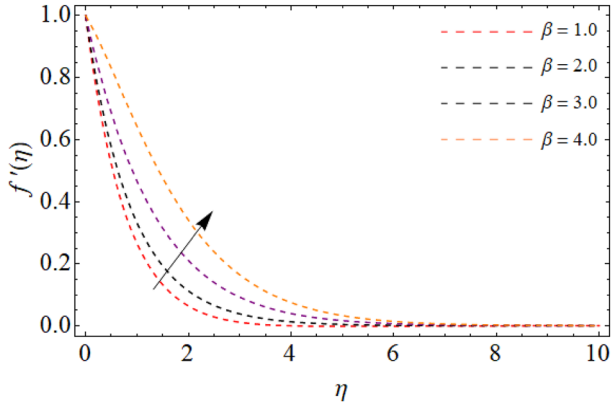

Figure 3. Velocity $f'(\eta)$ versus the third-grade fluid element β.

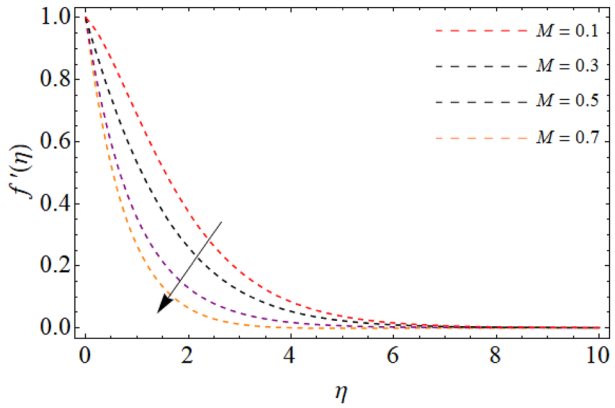

Figure 4. Fluid velocity $f'(\eta)$ versus magnetic term M.

chemical reaction effect augments the concentration field. Correspondingly, the significance of Sc controls the mass transfer, because the kinetic viscosity improves, which lessens the mass $\phi(\eta)$ outline as discovered in Fig. 12. The amount of the chemical reaction has a direct impact on the intensity of mass transfer, because it makes fluid atoms move more quickly, which causes the mass gradient $\phi(\eta)$ to rise as publicized in Fig. 11.

Table 3 disclosed the numerical outputs for skin friction $f''(0)$, Sherwood number $-\phi'(0)$ and Nusselt number $-\theta'(0)$. It has been noticed that the Nusselt number and Skin friction rises for the mounting values of Schmidth number.

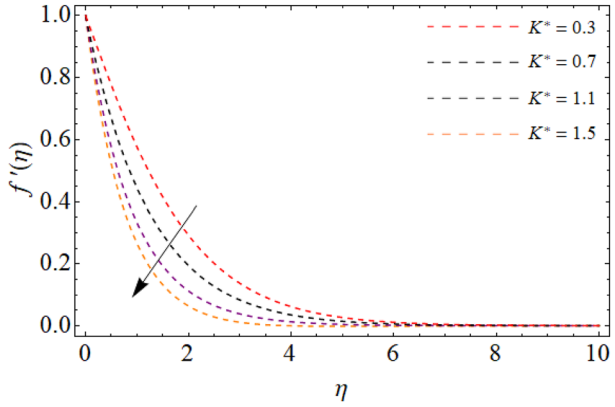

Figure 5. Fluid velocity $f'(\eta)$ versus permeability factor K^*.

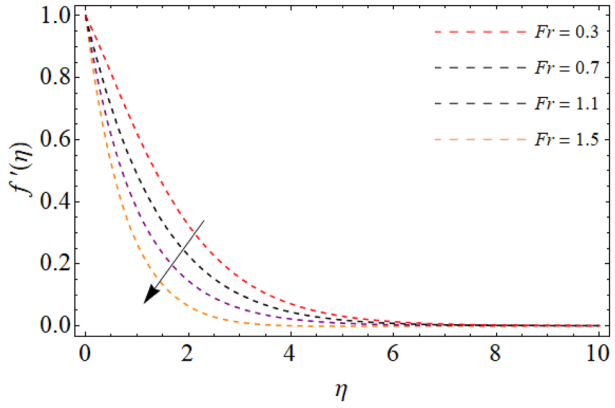

Figure 6. Fluid velocity $f'(\eta)$ versus inertial term Fr.

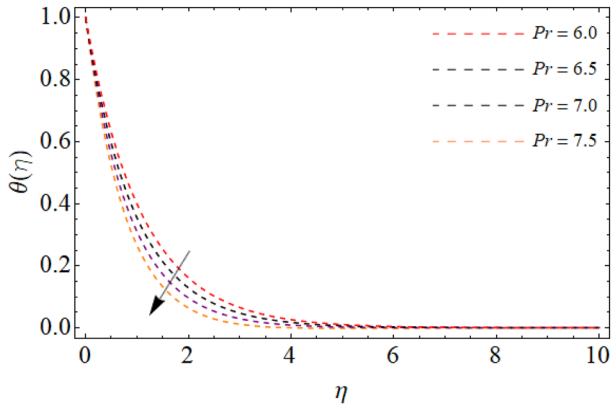

Figure 7. Fluid energy sketch $\theta(\eta)$ versus Prandtl number Pr.

Conclusions

We have numerically calculated the energy and mass transmission through the third-grade fluid and relation of the Darcy–Forchheimer across a stretching sheet. Additionally, the consequences of heat source, thermal radiation and magnetic effect are also studied with the fluid flow. The simplified set of ODEs is numerically resolved through the bvp4c technique, by using Mathematica software. The main findings are:

- Velocity curve enhances for the rising values of Richardson number Ri and third-grade fluid factor.

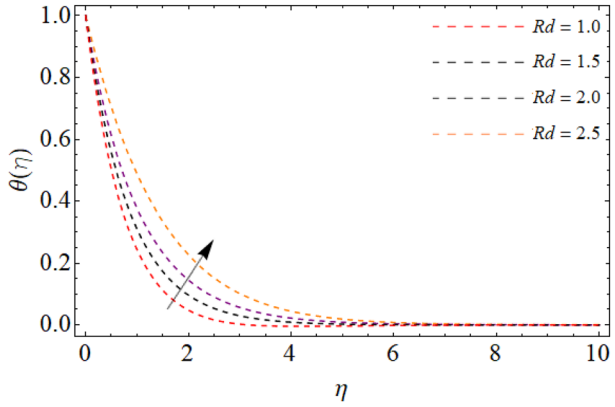

Figure 8. Fluid energy sketch $\theta(\eta)$ versus thermal radiation Rd.

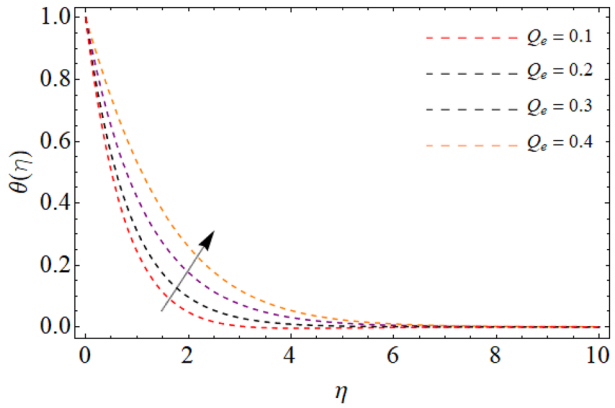

Figure 9. Fluid energy sketch $\theta(\eta)$ versus Heat source Q_e.

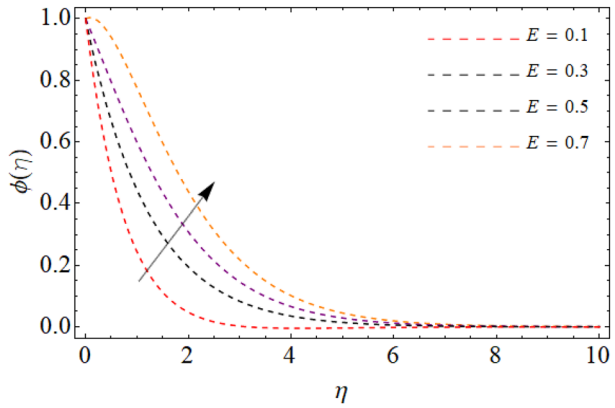

Figure 10. Fluid concentration sketch $\phi(\eta)$ versus Activation energy E.

- The influence of magnetic factor M, permeability factor K^* and local inertial constant Fr, all diminish the fluid velocity.
- The temperature curve drops with the effect of Prandtl number.
- The radiation effect transfers thermal energy form heat source to the system, which results in the elevation of energy field $\theta(\eta)$.
- The heat source working as heating agent for the flow system, there effect rises the fluid temperature $\theta(\eta)$.
- The consequence of chemical reaction boosts the concentration field, while declines with the Schmidth number.

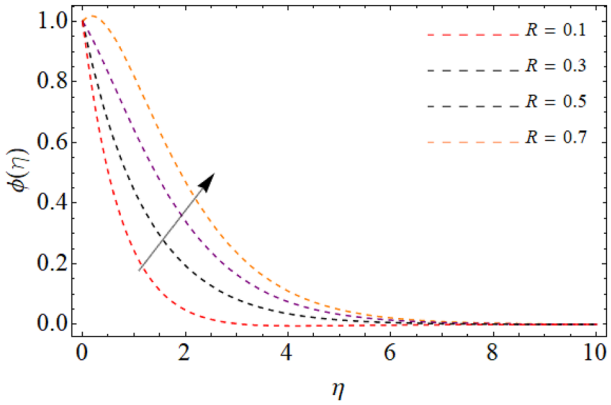

Figure 11. Fluid concentration sketch $\phi(\eta)$ versus chemical reaction R.

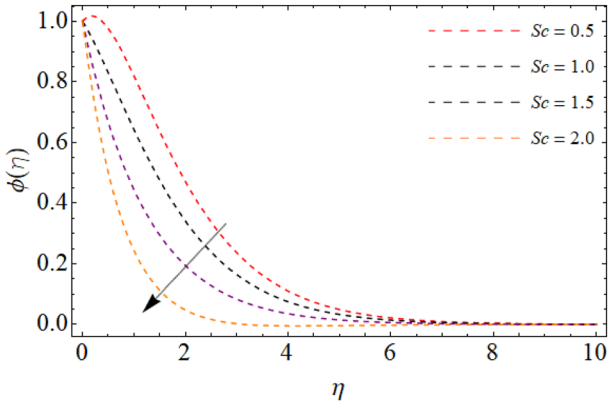

Figure 12. Fluid concentration sketch $\phi(\eta)$ versus Schmidth number Sc.

N	$f''(0)$	$-\theta'(0)$	$-\phi'(0)$
0.3	1.5047730457472	2.7930245333898	0.3804378693486
0.5	0.6521245649586	3.0398628093226	0.4354683514387
0.7	−0.5760489752623	3.3020406132527	0.4897833078565
0.9	−1.3605022868920	3.4249212406151	0.5160047901888
Sc	–	–	–
0.1	1.5047730547472	2.7930245333898	0.3804378693486
0.2	1.5153784960713	2.7861051786865	1.3656576445162
0.3	1.5244263887091	2.7814596692455	2.3837736504415
0.4	1.5280410380701	2.7799706702532	2.8994715445831

Table 3. The numerical outputs for skin friction $f''(0)$, Sherwood number $-\phi'(0)$ and Nusselt number $-\theta'(0)$.

Data availability

All data used in this manuscript have been presented within the article.

Received: 24 March 2023; Accepted: 31 October 2023
Published online: 10 November 2023

References:

1. Abolbashari, M. H., Freidoonimehr, N., Nazari, F. & Rashidi, M. M. Analytical modeling of entropy generation for Casson nano-fluid flow induced by a stretching surface. *Adv. Powder Technol.* **26**(2), 542–552 (2015).
2. Zeeshan, A., Majeed, A. & Ellahi, R. Effect of magnetic dipole on viscous ferro-fluid past a stretching surface with thermal radiation. *J. Mol. Liq.* **215**, 549–554 (2016).

3. Shit, G. C., Haldar, R. & Mandal, S. Entropy generation on MHD flow and convective heat transfer in a porous medium of exponentially stretching surface saturated by nanofluids. *Adv. Powder Technol.* **28**(6), 1519–1530 (2017).
4. Sandeep, N. & Sulochana, C. Momentum and heat transfer behaviour of Jeffrey, Maxwell and Oldroyd-B nanofluids past a stretching surface with non-uniform heat source/sink. *Ain Shams Eng. J.* **9**(4), 517–524 (2018).
5. Besthapu, P., Haq, R. U., Bandari, S. & Al-Mdallal, Q. M. Thermal radiation and slip effects on MHD stagnation point flow of non-Newtonian nanofluid over a convective stretching surface. *Neural Comput. Appl.* **31**, 207–217 (2019).
6. Alqahtani, A. M., Bilal, M., Ali, A., Alsenani, T. R. & Eldin, S. M. Numerical solution of an electrically conducting spinning flow of hybrid nanofluid comprised of silver and gold nanoparticles across two parallel surfaces. *Sci. Rep.* **13**(1), 7180 (2023).
7. Chu, Y. M. *et al.* Significance of activation energy, bio-convection and magnetohydrodynamic in flow of third grade fluid (non-Newtonian) towards stretched surface: A Buongiorno model analysis. *Int. Commun. Heat Mass Transfer* **118**, 104893 (2020).
8. Kumar Mishra, N. *et al.* Investigation of blood flow characteristics saturated by graphene/CuO hybrid nanoparticles under quadratic radiation using VIM: Study for expanding/contracting channel. *Sci. Rep.* **13**(1), 8503 (2023).
9. Li, Y. X. *et al.* Heat and mass transfer in MHD Williamson nanofluid flow over an exponentially porous stretching surface. *Case Stud. Therm. Eng.* **26**, 100975 (2021).
10. Khan, U., Waini, I., Ishak, A. & Pop, I. Unsteady hybrid nanofluid flow over a radially permeable shrinking/stretching surface. *J. Mol. Liq.* **331**, 115752 (2021).
11. Elattar, S. *et al.* Computational assessment of hybrid nanofluid flow with the influence of hall current and chemical reaction over a slender stretching surface. *Alex. Eng. J.* **61**(12), 10319–10331 (2022).
12. Dogonchi, A. S. *et al.* Thermal and entropy analyses on buoyancy-driven flow of nanofluid inside a porous enclosure with two square cylinders: Finite element method. *Case Stud. Therm. Eng.* **27**, 101298 (2021).
13. Mishra, S., Mahanthesh, B., Mackolil, J. & Pattnaik, P. K. Nonlinear radiation and cross-diffusion effects on the micropolar nanoliquid flow past a stretching sheet with an exponential heat source. *Heat Transfer* **50**(4), 3530–3546 (2021).
14. Mohanty, B., Jena, S. & Pattnaik, P. K. MHD nanofluid flow over stretching/shrinking surface in presence of heat radiation using numerical method. *Int. J. Emerg. Technol.* **10**(2), 119–125 (2019).
15. Pattnaik, P. K., Bhatti, M. M., Mishra, S. R., Abbas, M. A. & Bég, O. A. Mixed convective-radiative dissipative magnetized micropolar nanofluid flow over a stretching surface in porous media with double stratification and chemical reaction effects: ADM-Padé computation. *J. Math.* **2022**, 1–19 (2022).
16. Kumam, P., Anwar, T., Shah, Z. & Watthayu, W. Analysis and modeling of fractional electro-osmotic ramped flow of chemically reactive and heat absorptive/generative Walters' B fluid with ramped heat and mass transfer rates. *AIMS Math.* **6**(6), 5942–5977 (2021).
17. Saeed, A. *et al.* Fractional order stagnation point flow of the hybrid nanofluid towards a stretching sheet. *Sci. Rep.* **11**(1), 20429 (2021).
18. Bilal, M., Arshad, H., Ramzan, M., Shah, Z. & Kumam, P. Unsteady hybrid-nanofluid flow comprising ferrousoxide and CNTs through porous horizontal channel with dilating/squeezing walls. *Sci. Rep.* **11**(1), 1–16 (2021).
19. Massoudi, M. & Christie, I. Effects of variable viscosity and viscous dissipation on the flow of a third grade fluid in a pipe. *Int. J. Non-Linear Mech.* **30**(5), 687–699 (1995).
20. Ariel, P. D. Flow of a third grade fluid through a porous flat channel. *Int. J. Eng. Sci.* **41**(11), 1267–1285 (2003).
21. Ellahi, R. & Riaz, A. Analytical solutions for MHD flow in a third-grade fluid with variable viscosity. *Math. Comput. Modell.* **52**(9–10), 1783–1793 (2010).
22. Bilal, M., Ullah, I., Alam, M. M., Shah, S. I. & Eldin, S. M. Energy transfer in Carreau Yasuda liquid influenced by engine oil with Magnetic dipole using tri-hybrid nanoparticles. *Sci. Rep.* **13**(1), 5432 (2023).
23. Adesanya, S. O., Falade, J. A., Jangili, S. & Bég, O. A. Irreversibility analysis for reactive third-grade fluid flow and heat transfer with convective wall cooling. *Alex. Eng. J.* **56**(1), 153–160 (2017).
24. Reddy, G. J., Hiremath, A. & Kumar, M. Computational modeling of unsteady third-grade fluid flow over a vertical cylinder: A study of heat transfer visualization. *Results Phys.* **8**, 671–682 (2018).
25. Mahanthesh, B. & Joseph, T. V. Dynamics of magneto-nano third-grade fluid with Brownian motion and thermophoresis effects in the pressure type die. *J. Nanofluids* **8**(4), 870–875 (2019).
26. Pattnaik, P. K., Mishra, S. R. & Sharma, R. P. Numerical simulation for flow through conducting metal and metallic oxide nanofluids. *J. Nanofluids* **9**(4), 354–361 (2020).
27. Pattnaik, P. K., Pattnaik, J. R., Mishra, S. R. & Nisar, K. S. Variation of the shape of Fe_3O_4-nanoparticles on the heat transfer phenomenon with the inclusion of thermal radiation. *J. Therm. Anal. Calorim.* **147**(3), 2537–2548 (2022).
28. Anwar, T., Kumam, P. & Watthayu, W. Unsteady MHD natural convection flow of Casson fluid incorporating thermal radiative flux and heat injection/suction mechanism under variable wall conditions. *Sci. Rep.* **11**(1), 4275 (2021).
29. Anwar, T., Kumam, P., Baleanu, D., Khan, I. & Thounthong, P. Radiative heat transfer enhancement in MHD porous channel flow of an Oldroyd-B fluid under generalized boundary conditions. *Phys. Scr.* **95**(11), 115211 (2020).
30. Anwar, T., Kumam, P., Khan, I. & Thounthong, P. Fractional magnetohydrodynamic flow of a second grade fluid in a porous medium with variable wall velocity and Newtonian heating. *Fractals* **29**(03), 2150060 (2021).
31. Al-Habahbeh, O. M., Al-Saqqa, M., Safi, M. & Khater, T. A. Review of magnetohydrodynamic pump applications. *Alex. Eng. J.* **55**(2), 1347–1358 (2016).
32. Rashidi, S., Esfahani, J. A. & Maskaniyan, M. Applications of magnetohydrodynamics in biological systems—A review on the numerical studies. *J. Magn. Magn. Mater.* **439**, 358–372 (2017).
33. Ellahi, R., Alamri, S. Z., Basit, A. & Majeed, A. Effects of MHD and slip on heat transfer boundary layer flow over a moving plate based on specific entropy generation. *J. Taibah Univ. Sci.* **12**(4), 476–482 (2018).
34. Lv, Y. P. *et al.* Numerical approach towards gyrotactic microorganisms hybrid nanoliquid flow with the hall current and magnetic field over a spinning disk. *Sci. Rep.* **11**(1), 1–13 (2021).
35. Kumam, P., Shah, Z., Watthayu, W. & Anwar, T. Radiative MHD unsteady Casson fluid flow with heat source/sink through a vertical channel suspended in porous medium subject to generalized boundary conditions. *Phys. Scr.* **96**(7), 075213 (2021).
36. Tian, M. W., Rostami, S., Aghakhani, S., Goldanlou, A. S. & Qi, C. A techno-economic investigation of 2D and 3D configurations of fins and their effects on heat sink efficiency of MHD hybrid nanofluid with slip and non-slip flow. *Int. J. Mech. Sci.* **189**, 105975 (2021).
37. Bhatti, M. M., Arain, M. B., Zeeshan, A., Ellahi, R. & Doranehgard, M. H. Swimming of Gyrotactic Microorganism in MHD Williamson nanofluid flow between rotating circular plates embedded in porous medium: Application of thermal energy storage. *J. Energy Storage* **45**, 103511 (2022).
38. Alharbi, K. A. M. *et al.* Computational valuation of darcy ternary-hybrid nanofluid flow across an extending cylinder with induction effects. *Micromachines* **13**(4), 588 (2022).
39. Hamid, A. & Khan, M. Impacts of binary chemical reaction with activation energy on unsteady flow of magneto-Williamson nanofluid. *J. Mol. Liq.* **262**, 435–442 (2018).
40. Shamshuddin, M. D., Mishra, S. R., Bég, O. A. & Kadir, A. Numerical study of heat transfer and viscous flow in a dual rotating extendable disk system with a non-Fourier heat flux model. *Heat Transf. Asian Res.* **48**(1), 435–459 (2019).
41. Kumam, P., Tassaddiq, A., Watthayu, W., Shah, Z. & Anwar, T. Modeling and simulation based investigation of unsteady MHD radiative flow of rate type fluid; a comparative fractional analysis. *Math. Comput. Simul.* **201**, 486–507 (2022).

42. Khan, M. I. & Alzahrani, F. Binary chemical reaction with activation energy in dissipative flow of non-Newtonian nanomaterial. *J. Theor. Comput. Chem.* **19**(03), 2040006 (2020).
43. Adnan, & Ashraf, W. Joule heating and heat generation/absorption effects on the heat transfer mechanism in ternary nanofluid containing different shape factors in stretchable converging/diverging Channel. *Waves Random Complex Media* https://doi.org/10.1080/17455030.2023.2198038 (2023).
44. Li, S. *et al.* Effects of activation energy and chemical reaction on unsteady MHD dissipative Darcy-Forchheimer squeezed flow of Casson fluid over horizontal channel. *Sci. Rep.* **13**(1), 2666 (2023).
45. Abbas, A., Shafqat, R., Jeelani, M. B. & Alharthi, N. H. Significance of chemical reaction and Lorentz force on third-grade fluid flow and heat transfer with Darcy-Forchheimer law over an inclined exponentially stretching sheet embedded in a porous medium. *Symmetry* **14**(4), 779 (2022).
46. Kumar, M. A. & Reddy, Y. D. Computational modelling of radiative Maxwell fluid flow over a stretching sheet containing nanoparticles with chemical reaction. *J. Indian Chem. Soc.* **100**(1), 100877 (2023).
47. Algehyne, E. A. *et al.* Gyrotactic microorganism hybrid nanofluid over a Riga plate subject to activation energy and heat source: numerical approach. *Sci. Rep.* **13**(1), 13675 (2023).
48. Raizah, Z., Alrabaiah, H., Bilal, M., Junsawang, P. & Galal, A. M. Numerical study of non-Darcy hybrid nanofluid flow with the effect of heat source and hall current over a slender extending sheet. *Sci. Rep.* **12**(1), 16280 (2022).
49. Mishra, N. K. *et al.* Numerical investigation of chemically reacting jet flow of hybrid nanofluid under the significances of bio-active mixers and chemical reaction. *Heliyon* **9**, e17678 (2023).
50. Magyari, E. & Keller, B. Heat and mass transfer in the boundary layers on an exponentially stretching continuous surface. *J. Phys. D Appl. Phys.* **32**(5), 577 (1999).

Acknowledgements

The authors present their appreciation to King Saud University for funding this research through Researchers Supporting Program number (RSPD2023R704), King Saud University, Riyadh, Saudi Arabia.

Author contributions

N.H.H. and M.B. wrote the manuscript and presented the numerical simulations. A.A. and S.M.E. thoroughly reviewed the mathematical calculation, M.S. and M.R. have thoroughly revised manuscript and restructured the manuscript. All authors are agreed on the final draft of the submission file.

Competing interests

The authors declare no competing interests.

Additional information

Correspondence and requests for materials should be addressed to M.U.R.

Reprints and permissions information is available at www.nature.com/reprints.

Publisher's note Springer Nature remains neutral with regard to jurisdictional claims in published maps and institutional affiliations.